CARBON-BASED NANOSTRUCTURE CREATED BY Ba AND Cs ATOMIC LAYER DEPOSITION ON THE VICINAL 3C-SiC(111) SURFACES

G.V. Benemanskaya[1,2*], P.A. Dementev[1], S.A. Kukushkin[2-4], M.N. Lapushkin[1],

A.V. Osipov[2,3], S.N. Timoshnev[2,5]

[1]Ioffe Institute, Politekhnicheskaya 26, St. Petersburg 194021, Russia

[2]Institute of Problems of Mechanical Engineering, Bolshoj pr. 61, Vas. Ostrov, St. Petersburg, 199178, Russia

[3]ITMO University, Kronversky pr. 49, St. Petersburg, 197101, Russia

[4]Peter the Great Saint-Petersburg Polytechnic University,

Politekhnicheskaya ul. 29, St. Petersburg, 195251, Russia

[5]Saint Petersburg National Research Academic University, Khlopina 8/3, St. Petersburg, 194021, Russia

*e-mail: Galina.Benemanskaya@mail.ioffe.ru

Abstract. New type of carbon based nanostructure on the vicinal 3C-SiC(111)-4° and 3C-SiC(111)-8° surfaces with adsorbed Ba and Cs nanolayers has been found. The 3C-SiC(111)-4° (8°) samples were grown by low-defect unstressed nanoscaled films epitaxy method on silicon vicinal substrates. Electronic structure of the 3C-SiC(111)-4° (8°) surfaces and the (Ba, Cs)/3C-SiC(111)-4° (8°) interfaces has been detailed studied *in situ* in an ultrahigh vacuum by synchrotron-based photoelectron spectroscopy. The C 1s, Si 2p, Ba 4d core levels and valence band spectra were investigated as a function of Ba or Cs submonolayer coverages. A special fine structure of the C 1s core level spectrum was revealed to appear under Ba and Cs adsorption on the vicinal SiC surface only. Drastic change in the C 1s spectrum was ascertained and shown to be originated from the interacting Si vacancy and adsorbed Ba (Cs) atoms initiating both the electron redistribution and surface reconstruction effects with formation of a new type of the C-enriched graphitic-like nanostructure.

Keywords: silicon carbide on silicon; wide bandgap semiconductors; thin film epitaxy; carbon-based nanostructure; vicinal 3C-SiC(111) surfaces; absorbed Ba and Cs nanolayers; electronic structure.
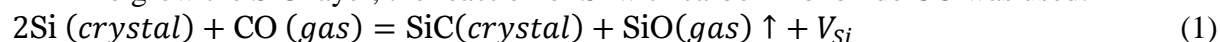
1. Introduction

During the last years, the physics and chemistry of silicon carbide (SiC) play an ever increasing role in the nanoelectronic, chemical functionalization and processing of such material, and it has been expanded to various new 2D inorganic materials.

One of the significant problems of micro- and optoelectronics is to grow the high-quality wide-band gap semiconductor films of SiC. Silicon carbide is a very remarkable candidate for electronic devices to be used under extreme conditions such as high temperature, voltage, power and frequency. Furthermore, SiC can be considered as promising material for biophysics applications owing to its low weight, high strength and extreme hardness [1-3].

Most of these applications are oriented toward thin film geometry. The main obstacle to grow the low-defective films on Si is the elastic stresses arising due to mismatch of the lattice

parameters of SiC layer and silicon substrate. To obtain stress-free films of SiC, a original method was developed for the solid-phase synthesis of epitaxial layers when the substrate itself is involved into a chemical reaction and the reaction product is grown inside the substrate layer [4-6]. The epitaxial 3C-SiC layers, synthesized by the original method of chemical atom substitution, were free of the elastic stresses because of their relaxation due to the interaction of point defects arising during the chemical reaction.

To grow the SiC layer, the reaction of Si with carbon monoxide CO was used:

$$2\text{Si}\,(crystal) + \text{CO}\,(gas) = \text{SiC}(crystal) + \text{SiO}(gas) \uparrow + V_{Si} \qquad (1)$$

This reaction provides a formation of pair point defects in Si matrix – the silicon vacancies V_{Si} arising due to removed gaseous silicon monoxide, SiO, and the carbon atoms, C, turning out in the interstitial positions in Si crystal after oxygen loss. Then, each pair defect causes dilatation strain, i.e., they become dilatation centers in a cubic silicon crystal.

Formation of the silicon vacancies V_{Si} is accompanied by appearance of the C atoms in the Si lattice because CO molecule transfers one's atomic oxygen to silicon. Therefore such a point dilatation defects are generated by pairs. The strong mutual attraction between pairs caused by interaction with elastic field leads to formation of the relatively stable pair of the defects named by dilatation dipoles [5, 6] by analogy with electric dipoles, providing significant reduction of the total elastic energy. It is eliminated that the most favorable position of the dipoles is the (111) direction in crystals with cubic symmetry. Assembly of dilatation dipoles provides relatively overall relaxation of elastic stress induced by disagreement of Si and SiC lattices.

The integration of new-grown SiC nanolayers into silicon technology requires studies of surface properties, and in particular, the interface formation. Surface electronic properties of SiC grown by traditional method and especially by a new method are still poorly understood and then they cause discussion relative to interface formation, surface state spectra, band-bending, and the effect of 2D phase transition. This is important because of a pivotal role that such properties play in nanostructure research where these surface and interface conditions are crucial. However, the surface and interface electronic structure of silicon carbide is not completely understood.

An effective tool to investigate electronic structure of both the semiconductor bulk and surface is photoelectron spectroscopy (PES). The electronic structure of SiC, grown by traditional method, has been a subject of the number of experimental [7-15] and theoretical [16-21] investigations. The surface related features were obtained by PES and X-ray photoelectron spectroscopy and shown to be correlated to the Si dangling bonds and interaction between the top Si atoms and C atoms [7-9, 13-14]. Calculations based on the density functional theory within the local density approximation have predicted such peculiarities [17, 20, 21]. Moreover, these theoretical studies show that the surface electronic structure corresponding to the occupied states below the Fermi level could be explained by Si-dangling bonds of SiC surface [20, 21].

Adsorbed alkali-metal layers are good candidates for metal-semiconductor interface formation and Schottky barrier composition. Electronic properties of surfaces and interfaces were most thoroughly studied for hexagonal 6H-SiC(0001) surfaces. With respect to Cs/6H-SiC interface the Cs-induced donor states belonging to Cs-Si bonds were obtained together with the semiconducting-like character of interface [22]. The Schottky barrier formation and interfacial chemistry were studied for the Sc/3C-SiC(111) interface [23]. The upward band bending of ~ 0.5 eV and Schottky barrier of ~ 0.7 eV were obtained. Electronic properties were investigated for interfaces consisting of Si(110) face and 3C-SiC (111) face [24]. The coexistence of the floating bonds and the Si dangling bonds with the electron transfer was revealed as the mechanism of the stabilization of the interface.

Recently, formation of the Cs, Ba/3C-SiC(111) interfaces in the case of flat surfaces was investigated as a function of coverage with the use of PES [25, 26]. The plane face 3C-SiC(111)

samples were grown by the method of epitaxy of low-defect unstressed nanoscaled silicon carbide films. Valence band photoemission and both the Si 2p and C 1s core levels spectra have been investigated as a function of submonolayer coverage. Under Ba and Cs adsorption two surface bands induced by adsorption are found. It is obtained that interfaces can be characterized as metallic-like. Modification of the Si 2p and C 1s surface-related components was ascertained and shown to be provided by redistribution effect of electron density between adatoms and both the Si surface and C interface atoms.

A number of articles are focused on the effects of metal or nitrogen adsorption on graphene grown on SiC surfaces [27-31]. Adsorption Cs, Rb has been explored in detail on graphene and shown that adatoms deposited on monolayer graphene samples gives rise to *n*-type doping with electron transfer from the metal to the graphene layer [27]. It is obtained that the Na atoms can intercalate into the space between the graphene and the buffer layer [28]. Returning to the study of SiC surfaces, it can be noted that the electronic properties of 3C-SiC(111) surface are less studied in contrast to the well investigated SiC(100) and SiC(0001) ones. Vicinal surfaces of SiC and metal adsorption on those surfaces are also almost completely unexplored. Nevertheless these issues are of great importance from both fundamental and applied points of view. The vicinal surfaces can be useful in facilitating stress relaxation due to significant mismatch of lattice constants at the initial stages of nucleation with the growth of nitrides on the SiC.

In this paper, the electronic structure of the vicinal 3C-SiC(111)-4° and the 3C-SiC(111)-8° surfaces grown by the original method has been first studied by PES. Atomic structure of the samples has been obtained by atomic-force microscopy (AFM). The modification of the electronic structure in the process of Cs and Ba adsorption on the vicinal 3C-SiC(111)-4° and the 3C-SiC(111)-8° surfaces was first studied. It is found drastic change in the C 1s core level and valence band spectra for the Ba, Cs/3C-SiC-4° and Ba/3C-SiC-8° interfaces as a function of Ba and Cs coverages.

2. Experimental

Vicinal 3C-SiC(111)-4° and 3C-SiC(111)-8° surface growth. The single-crystal epitaxial 3C-SiC(111)-4° layers have been grown on the vicinal Si(111)-4° and Si(111)-8° surfaces inclined at angles of 4° and 8°to the (111) base orientation. The 3C-SiC(111)-4° and 8° layers were synthesized by the method of chemical atom substitution [4-6]. The temperature in the synthesis zone was 1530 K; the total pressure of the gas mixture (CO + SiH$_4$) was 79 Pa; the flux rate of the gas mixture was 12 sccm; the silane (SiH$_4$) percentage in the flux of the mixture corresponded to 45 %. The epitaxial 3C-SiC(111)-4° and 3C-SiC(111)-8° layers were studied by X-ray diffraction (XRD) analysis, AFM, and the electron diffraction technique. The full width at half-maximum (FWHM$\omega - \beta$) of the XRD peak observed for the samples with Cu$K\alpha$1 radiation was 40 arcmin, which is indicative of the epitaxial orientation of the structures. The layers thickness was ~150 nm.

Figures 1 and 2 present the experimental data that are characterized the morphology of the 3C-SiC(111)-4° sample as a typical case for all samples studied here. Structure of SiC samples was ascertained by scanning electron microscopy (SEM), as can be seen in Fig. 1. Surface morphology of the samples was characterized by AFM, see Fig. 2.

PES experiments. Photoemission studies were carried out at BESSY II, Helmholtz Zentrum, Berlin using the synchrotron radiation with photon energies in the range of 120–450 eV. PES experiments were performed in an ultrahigh vacuum of 5x10^{-10} Torr at room temperature. The SiC samples were preliminary heated at a temperature of ~ 900 K. The spectra were collected in normal emission. For the 3C-SiC(111)-4° and the 3C-SiC(111)-8° samples the photoemission spectra from the valence band (VB), from the surface states and from the C 1s, Ba 4d, Cs 5p core levels were recorded. The main elements presented in PES overview of

the clean SiC were Si, C and negligible O and no other elements were detected in significant amounts. A total energy resolution of better than 100 meV was used.
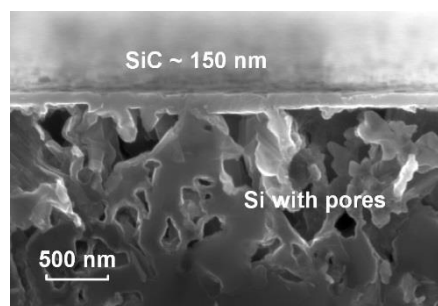

Fig. 1. SEM cross-section of 3C-SiC(111)-4° layer of thickness ~150 nm grown on the vicinal Si(111)-4° substrate.
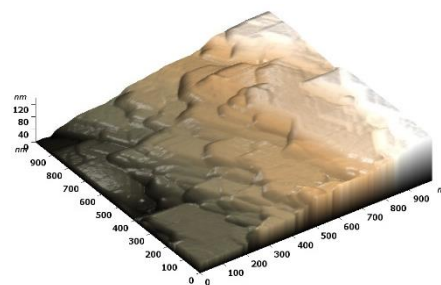

Fig. 2. AFM 3D image of a 1x1 μm region of the vicinal 3C-SiC(111)-4° surface.

Atomically pure cesium or barium were deposited onto the clean samples from a standard sources. Step-by-step deposition of Ba or Cs coverages was performed onto the 3C-SiC(111)-4° and the 3C-SiC(111)-8° samples. It should be noted that the Ba sticking coefficient is equal to one at least up to 1 monolayer (ML). To ascertain the Cs or Ba coverage, the sources were preliminary calibrated to dosage using the original technique [32]. This made possible to determine Ba and Cs coverages deposited onto the samples to better than 20%. Note that 1 ML is defined as one complete layer of Ba (Cs) atoms and equal to $\sim 6 \times 10^{14}$ atoms/cm^2 [33]. Moreover, the Ba (Cs) overlayer corresponding to 1 ML can be estimated using dependence of the Ba 4d and Cs 5p core level peak intensities as a function of the Ba (Cs) deposition time [34, 35]. It should be noted that we deal with rough surfaces which are remarkable for steps and buckling. Therefore, it should be indicated as a relative 1 ML coverage.

3. Results and discussion

Figure 3 represents the C 1s core level spectra taken from the clean 3C-SiC(111)-4° surface (Fig. 3a) and from the Ba/3C-SiC(111)-4° interface at different Ba coverages (Fig. 3b, c). The exciting photon energy corresponds to $hv = 450$ eV. The C 1s core level spectrum for the clean SiC surface is found to be composed of two distinct components B and S1 (Fig. 3a). The one at the energy of 283.1 eV (peak B) is originated from the bulk of SiC substrate and the other one S1 at the higher binding energy (285.0 eV) then bulk component B can be assigned to the surface C-C bond. In agreement with the observations [30-31], the component S1 is related to the presence of s-p^2 hybridized C-C bonds. This peak S1 can be considered as a signature of the C-enriched surface.

Drastic change in the C 1s core level spectrum was found for the Ba/3C-SiC(111)-4° interface (Fig. 3b, c). The appearance of additional component S2 at the higher binding energy (286.5 eV) was revealed as an effect of Ba adsorption at 0.5 ML and 1.0 ML. Simultaneously with the S2 peak, the additional peak SU on the highest binding energy (291.0 eV) arises. The binding energies of S2 and SU components does not depend on the coverage, only the relative intensities being equally modified throughout the increase of Ba coverage. On the other hand, several components appear at the higher binding energies indicating a stronger degree of interaction between C-C atoms and increase of the C ionicity. The presence of S1 and S2 components is widely identified a corrugation of the vicinal 3C-SiC(111)-4° surface.

An extremely unusual C 1s spectrum was found upon one monolayer of Ba adsorption on the 3C-SiC(111)-4° surface (Fig. 3c). Namely, a supplementary peak SU was distinctly found. One should note that both the S2 and SU components synchronously arise and increase in intensities with Ba coverage. This marked peculiarity SU, which differs from the traditional

C 1*s* core level spectrum, can be identified as a shake-up satellite of the peak S2. The shake-up satellite is a well established characteristic of the photoemission process in graphitic and aromatic systems. The shake-up is a two electron phenomenon; the emitted photoelectrons with energy S2 (286.0 eV) can excite a transition resulting in an additional peak SU (291.0 eV) at the higher binding energy. Graphitic systems show a shake-up peak shifted toward higher binding energy from the main peak by approximately 6.5–7.0 eV [36, 37]. Therefore the modification of surface structure of the vicinal 3C-SiC(111)-4° surface due to Ba adsorption was obtained with the formation of apparently the missing-row reconstruction. It is found that surface phase transition from the 3C-SiC(111)-4° C-enriched surface to graphitic-like one is originated from the Ba adsorption.
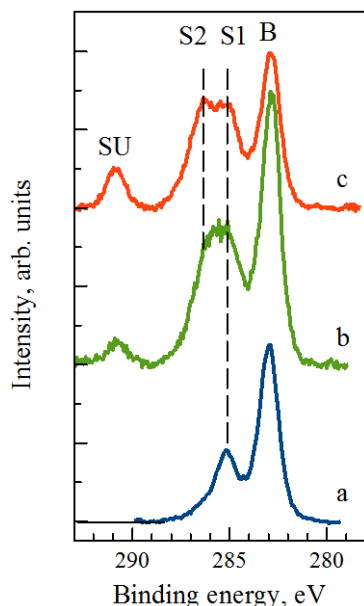

Fig. 3. Photoemission spectra of C 1*s* core level for Ba/3C-SiC(111)-4° interface at different Ba coverages: (a) clean surface, (b) 0.5 ML, (c) 1.0 ML. Excitation energy *hν* = 450 eV.
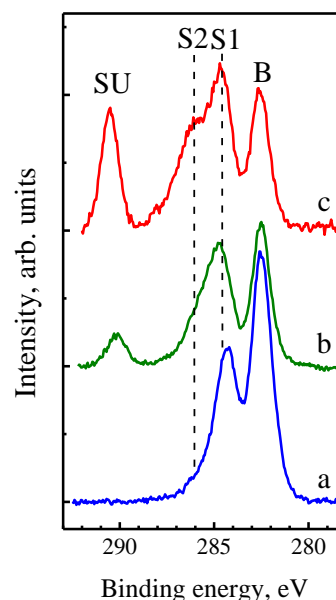
Fig. 4. Photoemission spectra of C 1*s* core level for Ba/3C-SiC(111)-8° interface at different Ba coverages: (a) clean surface, (b) 0.4 ML, (c) 1.0 ML. Excitation energy *hν* = 450 eV.

Figure 4 represents the C 1*s* core level spectra taken from the clean 3C-SiC(111)-8° surface (Fig. 4a) and from the Ba/3C-SiC(111)-8° interface at different Ba coverages (Fig. 4b, c). The exciting photon energy corresponds to *hν* = 450 eV. The C 1*s* core level spectrum for the clean 3C-SiC(111)-8° surface is found to be composed of two distinct components B and S1 (Fig. 4a). The B peak at the energy of 282.6 eV can be originated from the bulk substrate and the other one S1 at the higher binding energy (284.8 eV) with respect to B peak can be assigned to the surface C-C bond and the C-enriched surface.

An extraordinary C 1*s* spectrum was found upon Ba adsorption on the 3C-SiC(111)-8° surface (Fig. 4 b, c). As can be seen, the spectra for Ba/3C-SiC(111)-8° interface (Fig 4) are very similar to the Ba/3C-SiC(111)-4° interface (Fig. 3). Thus, for both cases of vicinal surfaces, the Ba adsorption on the 3C-SiC(111)-4°, (8°) surfaces causes the 2D phase transition from the carbon-enriched surface to the graphitic-like one with the formation of apparently the missing-row reconstruction.

Figure 5 represents drastic change in the C 1*s* core level spectra initiated by the Cs adsorption on the vicinal 3C-SiC(111)-4° surface. The exciting photon energy corresponds to *hν* = 450 eV. It is evident from the comparison of Fig. 5 with Figs. 3 and 4 that both the Cs and

Ba adatoms strongly and in a similar manner interact with the initially C-enriched vicinal surfaces. Therefore, unusual and complex structure of C 1s core level spectra was found upon Ba and Cs adsorption. This effect is originated from the strong interaction of the Ba (Cs) adatoms with C-surface atoms that causes the 2D structural phase transition leading to the formation of the missing-row reconstruction with the graphitic-like surface.
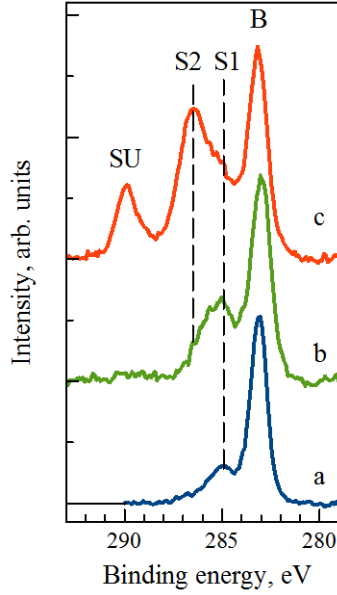

Fig. 5. Photoemission spectra of C 1s core level for Cs/3C-SiC(111)-4° interface at different Cs coverages: (a) clean surface, (b) 0.3 ML, (c) 1.0 ML. Excitation energy $hv = 450$ eV.
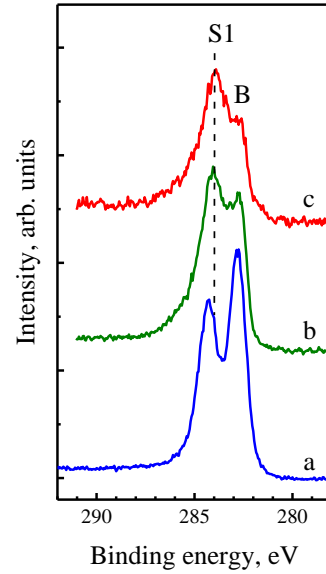
Fig. 6. Photoemission spectra of C 1s core level for Ba/3C-SiC(111) interface at different Ba coverages: (a) clean surface, (b) 0.6 ML, (c) 1.0 ML. Excitation energy $hv = 450$ eV.

Figure 6 shows photoemission spectra of the C 1s core level obtained for the flat 3C-SiC(111) surface (Fig. 6a) and for the Ba adsorption at different Ba coverages (Fig. 6 b, c). The C 1s core level for the clean flat SiC surface is found to be composed of two main components: the bulk component B and one shifted component S1 at lower binding energy. In agreement with the observations [30-31], the component S1 is related to the presence of s-p^2 hybridized C-C bonds. This peak S1 can be considered as a signature of the C-enriched surface.

Upon Ba adsorption all components B and S1 are decreased in intensity. Comparison of Fig. 6 and Figs. 3 and 4 clearly shows the essential difference in the C 1s core level spectra for the flat and vicinal SiC(111) surfaces. There are no additional components in the C 1s core level spectrum as compared to vicinal SiC surfaces. The C-based new structure can be created by the Ba and Cs adsorption.

Figure 7 presents the Ba 4d and Si 2p core level spectra for the Ba/3C-SiC(111)-4° interface. For the clean surface, dominant peak of the Si 2p is obtained. Upon Ba adsorption it is practically unchanged that is indicate about no interaction Si atoms with Ba atoms and absence of Si atoms in top surface layer. Other behavior can be seen for the Ba 4d core level spectra that arise and strongly increase in intensity with growing of the Ba coverage.

The photoemission spectra in the valence band region of Ba/3C-SiC(111)-4° interface are shown in Fig. 8 for the cases of a clean surface (a), and for Ba adsorption: 0.3 ML (b) and 1.0 ML coverage (c). The excitation photon energy is $hv = 120$ eV. The spectra are brought to the energy of the VB top at the surface, E_{VBM}. This energy is determined from linear approximation of the low-energy edge of the spectrum.
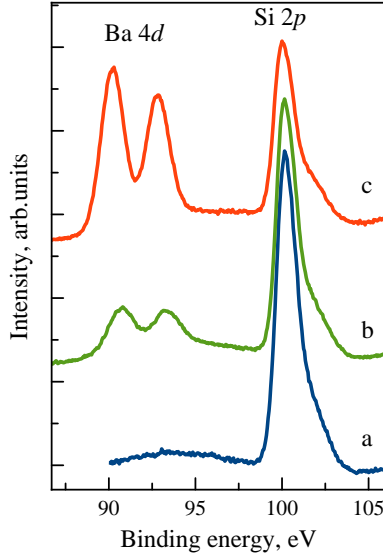
Fig. 7. Photoemission spectra of Ba 4*d* and Si 2*p* core levels for Ba/3C-SiC(111)-4° interface at different Ba coverages: a – clean surface, b – 0.3 ML, c – 1.0 ML. The excitation energy *hv* = 120 eV.
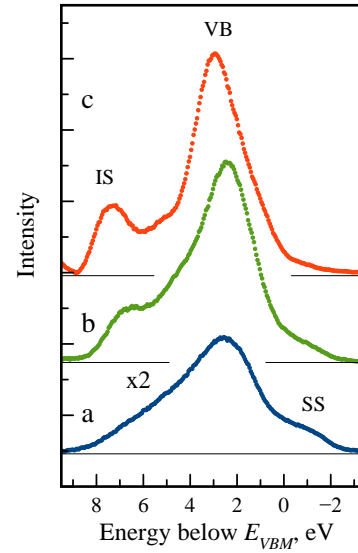
Fig. 8. Normal photoemission spectra in the VB region for Ba/3C-SiC(111)-4° interface at different Ba coverages: a – clean surface, b – 0.3 ML, c – 1.0 ML. The excitation energy *hv* = 120 eV.

For the clean 3C-SiC(111)-4° sample, the spectrum presents a slightly structured photoemission band with the width of ~8 eV. The maximum at the energy of ~2.5 eV corresponds to the photoemission from the VB. This inference is supported by calculations of the density of states (DoS) [15, 21] as well as by experimental data [7, 9, 13]. The additional peak at the binding energy of ~ -1.5 eV above the E_{VBM} can be related to the intrinsic surface states (SS), whose origin is associated with the Si dangling bonds [16, 17].

As the Ba coverage is increased, we observe an appearance and increase in the intensity of photoemission from the induced surface state IS at energy of ~ 7.0 eV, which is indicative of an increase in the electron density (DoS). As can be seen from Fig. 3, the vicinal 3C-SiC(111)-4° surface exhibits C-enriched reconstruction involving C atoms at different spatial positions. Ba adsorption is found to drastic modify initial surface to graphitic-like surface structure. The lack of states in the band-gap is indicative of the semiconductor character of the Ba/3C-SiC(111)-4° interface at coverage of less than 1 ML.

4. Simulation

A model taking into account silicon vacancies is developed for the system of the vicinal 3C-SiC(111)-4° surface interacting with Cs adsorbed atoms to understand formation of a new C-based surface nanostructure. To modeling the Cs atom interaction with the structure of the silicon carbide containing silicon vacancies saturated cluster approach will be used, which allows to use the highly accurate density functional methods [38]. Any Si atom removed from an infinite crystal lattice of atoms of a cubic SiC. Then the cesium atom is positioned on the resulting free place. Thus cluster of atoms that are arranged to the Cs closer than 6.1 Å obtained, namely, the nearest 7 shells of neighbors of the extracted atom (exactly 42 Si atoms and 42 C atoms) are taken into account. To minimize the cluster boundary influence the dangling bonds are saturated with hydrogen atoms. The geometry optimization of the system was carried out by methods of quantum mechanics, i.e. cluster configuration has been found, which corresponds to the energy minimum. It was assumed that only the Cs atom and nearest 16 atoms can move (see Fig. 9).

The system energy calculations were made with the density functional method, in particular, the hybrid functional B3LYP, which established himself as one of the most high-precision methods for problems of this type. Minimization of the functional was performed in the basis 6-31G++ [38], and appropriate pseudopotential used for cesium [23]. The energy minimization was performed in ORCA (https://orcaforum.cec.mpg.de/) and Gamess packages (http://www.msg.ameslab.gov/ GAMESS/index.html).
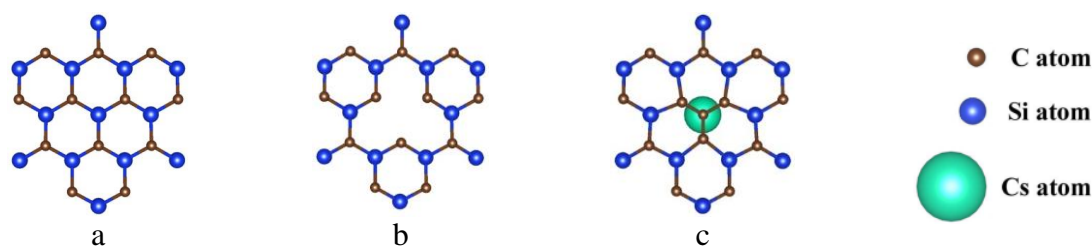

Fig. 9. Scheme of plane and atom arrangements for: (a) 3C-SiC(111) surface, (b, c) 3C-SiC(111) reconstructed surface and Cs atom interacting with Si-vacancy.

The optimization results of the system geometry are as follows. One of the 4 nearest to the Si-vacancy carbon atoms is profitably to take the place of silicon vacancy. The cesium atom is attached to the resulting almost flat cluster of 4 carbon atoms by means of a very short and strong ionic bond ~ 1.1 Å. In this case, cesium atom strongly pushes the remaining nearest 12 neighbors (see Fig. 9). It should be noted that if this structure is removed CsC_4 of 3C-SiC(111) crystal, the bond length between Cs and C atoms will increase by 3 times, namely, this structure can exist within the 3C-SiC(111) crystal only.

5. Conclusions

To summarize, the Ba/3C-SiC(111)-4°, Ba/3C-SiC(111)-8° and Cs/3C-SiC(111)-4° interfaces have been first investigated *in situ* using photoelectron spectroscopy with photon energies in the range of 120–450 eV. The vicinal 3C-SiC(111)-4° and 3C-SiC(111)-8° samples were grown by the original method of epitaxy of low-defect unstressed nanoscaled silicon carbide films. The C 1*s*, Si 2*p*, Ba 4*d* core levels and valence band photoemission spectra were obtained as a function of Ba and Cs submonolayer coverage. A special fine structure of the C 1*s* core level spectrum was revealed to appear under Ba or Cs adsorption on the vicinal surface exclusively. The drastic change in the C 1*s* core level spectrum is found to originate from the interacting silicon vacancy and adsorbed Cs or Ba atoms initiating electron redistribution effect which leads to the 2D phase transition from the 3C-SiC(111)-4° (8°) carbon-enriched surface to the graphitic-like one. It is found that Ba and Cs adsorption causes a charge transfer with increasing ionicity of the C surface atoms. In the valence band region, two surface bands induced by Ba adsorption are found to appear.

References

[1] S.E. Saddow, A.K. Agrawal, *Advances in silicon carbide processing and applications* (Artech House Publishers, London, 2004).
[2] P.G. Soukiassian, H.B. Enriquez // *Journal of Physics: Condensed Matter* **16** (2004) 1611.
[3] T. Seyller // *Journal of Physics: Condensed Matter* **16** (2004) 1755.
[4] S.A. Kukushkin, A.V. Osipov // *Journal of Physics D: Applied Physics* **47** (2014) 313001.
[5] S.A. Kukushkin, A.V. Osipov, N.A. Feoktistov // *Physics of the Solid State* **56** (2014) 1507.

[6] S.A. Kukushkin, A.V. Osipov // *Journal of Applied Physics* **113** (2013) 024909.

[7] L.I. Johansson, F. Owman, P. Mårtensson, C. Persson, U. Lindefelt // *Physical Review B* **53** (1996) 13803.

[8] V.M. Bermudez, J.P. Long // *Applied Physics Letters* **66** (1995) 475.

[9] H.W. Yeom, Y.-C. Chao, I. Matsuda, S. Hara, S. Yoshida, R.I.G. Uhrberg // *Physical Review B* **58** (1998) 10540.

[10] L.I. Johansson, F. Owman, P. Mårtensson // *Physical Review B* **53** (1996) 13793.

[11] R. Takahashi, H. Handa, S. Abe, K. Imaizumi, H. Fukidome, A. Yoshigoe // *Japanese Journal of Applied Physics* **50** (2011) 070103.

[12] J. Su, Q. Niu, C. Tang, Y. Zhang, Z. Fu // *Solid State Sciences* **14** (2012) 545.

[13] P.-A. Glans, T. Balasubramanian, M. Syväjärvi, R. Yakimova, L.I. Johansson // *Surface Science* **470** (2001) 284.

[14] C. Virojanadara, M. Hetzel, L.I. Johansson, W.J. Choyke, U. Starke // *Surface Science* **602** (2001) 525.

[15] C.H. Park, B.-H. Cheong, K.-H. Lee, K.J. Chang // *Physical Review B* **49** (1994) 4485.

[16] C. Persson, U. Lindefelt // *Journal of Applied Physics* **82** (1997) 5496.

[17] P. Käckell, B. Wenzien, F. Bechstedt // *Physical Review B* **50** (1994) 10761.

[18] J. Furthmüller, F. Bechstedt, H. Hüsken, B. Schröter, W. Richter // *Physical Review B* **58** (1998): 13712.

[19] F. Bechstedt, J. Furthmüller // *Journal of Physics: Condensed Matter* **16** (2004) 1721.

[20] Y. Li, X. Wang, L. Ye // *Journal of Physics: Condensed Matter* **18** (2006) 6953.

[21] J. Wang, L. Zhang, Q. Zeng, G.L. Vignoles, L. Cheng, A. Guette // *Physical Review B* **79** (2009) 125304.

[22] V. Elsbergen, T.U. Kampen, W. Mönch // *Journal of Applied Physics* **79** (1996) 316.

[23] S.W. King, R.J. Nemanich, R.F. Davis // *Physica Status Solidi B* **252** (2015) 391.

[24] E.K.K. Abavare, J.-I. Iwata, A. Oshiyama // *Physical Review B* **87** (2013) 235321.

[25] S.A. Kukushkin, G.V. Benemanskaya, P.A. Dementev, S.N. Timoshnev, B.Senkovskiy // *The Journal of Physical Chemistry* **90** (2016) 40.

[26] G.V. Benemanskaya, P.A. Dementev, S.A. Kukushkin, M.N. Lapushkin, A.V. Osipov // *Semiconductors* **50** (2016) 1327.

[27] S. Watcharinyanon, C. Virojanadara, L.I. Johansson // *Surface Science* **605** (2011) 1918.

[28] S. Watcharinyanon, L.I. Johansson, C. Xia, C. Virojanadara // *Journal of Applied Physics* **111** (2012) 083711.

[29] S.D. Costa, J.E. Weis, O. Frank, M. Kalbac // *Carbon* **93** (2015) 793.

[30] Z.-H. Sheng, L. Shao, J.-J. Chen, W.-J. Bao, F.-B. Wang, X.-H. Xia // *ACS Nano* **5** (2011) 4350.

[31] Y. Wang, Y. Shao, D.W. Matson, J. Li, Y. Lin // *ACS Nano* **4** (2010) 1790.

[32] G.V. Benemanskaya, G.E. Frank-Kamentskaya, N.M. Shmidt, M.S. Dunaevskiy // *Journal of Experimental and Theoretical Physics* **103** (2006) 441.

[33] C.-P. Cheng, I.-H. Hong, T.-W. Pi // *Physical Review B* **58** (1998) 4066.

[34] T. Okuda, K.-S. An, A. Harasawa, T. Kinoshita // *Physical Review B* **71** (2005) 085317.

[35] T.-W. Pi, I.-H. Hong, C.-P. Cheng // *Physical Review B* **58** (1998) 4149.

[36] L.B. Biedermann, M.L. Bolen, M.A. Capano, D. Zemlyanov, R.G. Reifenberger // *Physical Review B* **79** (2009) 125411.

[37] D. Briggs, J.T. Grant, *Surface Analysis by Auger and X-ray Photoelectron Spectroscopy* (IM Publications Chichester, UK and SurfaceSpectra, Manchester, UK, 2003).

[38] S.A. Kukushkin, A.V. Osipov // *Physics of the Solid State* **58** (2016) 747.